Zeitschrift: IABSE congress report = Rapport du congrès AIPC = IVBH Kongressbericht

Band: 12 (1984)

Artikel: Composite slab bridges using deformed flange T-shapes

Autor: Yamasaki, Tokuya / Kaneko, Tadao / Sato, Masakatsu

DOI: https://doi.org/10.5169/seals-12145

Composite Slab Bridges Using Deformed Flange T-shapes

Ponts-dalles mixtes utilisant des profilés en T à membrure déformée

Verbundplattenbrücken aus T-Trägern mit Formflansch

Tokuya YAMASAKI
Technical Adviser
Kawasaki Steel Corp.
Chiba, Japan

Tadao KANEKO
Manager
Kawasaki Steel Corp.
Chiba, Japan

Masakatsu SATO
Senior Researcher
Kawasaki Steel Corp.
Chiba, Japan

Tokuya Yamasaki, born 1922, got his Dr. degree in 1962, engaged as Prof. of structural engineering at Kyushu University, 1962–1971. From 1971 to 1982 he was General Manager and is now Technical Adviser at R&D Center of Kawasaki Steel Corp.

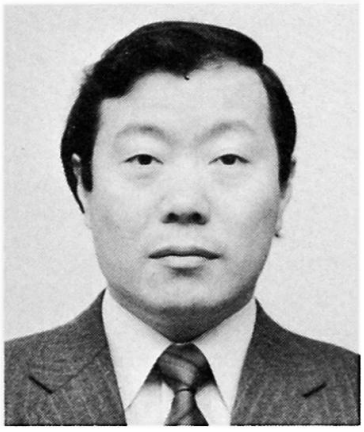

Tadao Kaneko, born 1943, got his Dr. degree in civil engineering at Kyushu University. Since 1972, he has studied the strength analysis of steel structures and is now senior researcher at R&D Center of Kawasaki Steel Corp.

Masakatsu Sato, born 1942, got his Dr. degree in analysis of composite girders at Tokyo University. For ten years he has been conducting research on composite and mixed structures at R&D Center of Kawasaki Steel Corp.

SUMMARY

Composite slab bridges made by filling up deformed flange T-shapes with concrete have been used for road bridges since 1982 in Japan. The structural characteristics of this bridge type have been investigated by conducting a high cycle fatigue test and a static bending rupture test. A design method is proposed.

RESUME

Les ponts-dalles mixtes — fabriqués en remplissant de béton des profilés en T à membrure déformée — sont utilisés au Japon depuis 1982, en tant que ponts routiers. Les caractéristiques structurales de ce type de pont ont été contrôlées au moyen d'essais de fatigue et d'essais statiques de rupture à la flexion. Une méthode de calcul est proposée.

ZUSAMMENFASSUNG

Verbundplattenbrücken, bestehend aus mit Beton gefüllten T-Profilen mit Formflansch, kommen seit 1982 in Japan als Strassenbrücken zur Anwendung. Das charakteristische Tragverhalten dieser Brücken konnte mit einem Ermüdungsversuch und einem statischen Biegebruchversuch bestätigt werden. Ein Bemessungsverfahren wird vorgestellt.

1. INTRODUCTION

Today, steel-concrete composite structures are widely used as materials for civil engineering and building because of a rational combination of the advantageous characteristics on steel and concrete; steel's tensile strength and toughness, concrete's compressive strength and stiffness, and composite structure's noise and vibration absorption and high corrosion resistance properties.

It is of primary importance that the steel-concrete composite structure be provided with an effective stress transmission mechanism in its steel-concrete interface. The bond strength between steel and concrete may be increased through either mechanical shear connectors, as used in composite girders, or surface projections as of deformed bar[1]. The latter has a great advantage in executive efficiency and material saving, and therefore, any substantial improvement in steel-concrete bond must be derived from the optimum selection of steel surface projections. In 1977, Kawasaki Steel corp. developed deformed flange H-shapes with lateral projections on the outside surface of both flanges, as shown in Fig. 1 for composite structures. The encased T girder in which the above-mentioned H-shapes were covered with expansive concrete and SRC piers in which these H-shapes were used instead of deformed bars were put to practical use in 1978 and 1979, respectively[2].

Recently, the authors have developed a new-type composite slab bridge made by filling up deformed flange T-shapes (cutting in half the new H-shapes) with expansive concrete. In this slab bridge, projections on the upper flange play the roll of shear connector to permit the concrete covering to make thinner. Therefore, the depth of this bridge can be made lower than that of coventional bridges. Further, the bottom plates can be utilized as permanent forms, thereby making it possible to achieve higher execution accuracy and reduce construction time.

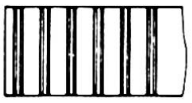

In this paper, the bond strength of deformed flange H-shapes to concrete are made clear. Then, the mechanical properties of this slab in the elastic range as well as the characteristics of constructional co-operation of steel girder and slab concrete at the failure stage are confirmed by conducting a high-cycle fatigue test and static bending rupture test on the approximately full-sized slab specimens. Finally, a design method is proposed for road bridges.

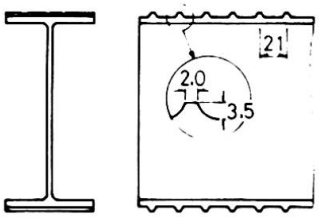

Fig. 1 Profile of deformed flange H

2. SELECTION OF PROJECTION SHAPES

2.1 Pull-out Tests for Flat and Lugged Steel Plates

The bond characteristics of lugged plates are considerably affected by such factors as height h, spacing d and setting angle θ of projection, and it has been empirically confirmed that the influence of θ is negligible when it is not less than 50°. In the present pullout tests where θ was set at 60° with h and d adopted as parameters, 17 sets of steel plates with lateral projections, including deformed flange plates of H-shapes, all of which are shown in Table 1, were used. The maximum size of aggregate coarse was 25 mm, and the

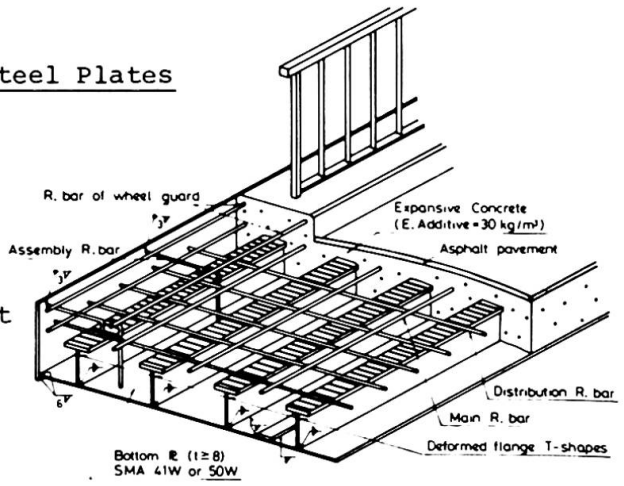

Fig. 2 Schema of composite slab bridges using deformed flange T-shapes

design strength of concrete was 29.4 MPa. Following four weeks of air curing, pull-out tests were performed to determine the relationship between bond stress τ_b and slip δ_f at the free end of test specimens.

2.2 Effect of Projections on Bond Stress

The relationship between τ_b and δ_f in pull-out tests is shown in Fig. 3 Bond strength of flat steel plate depends on inherent adhesion on the steel-concrete interface, such as agglutination and friction. Much of it is on the latter. Consequently, as the steel plate begins to slip, the amount of slip rises sharply to reach the maximum bond stress τ_{bmax}. On the other hand, lugged steel plates are designed to reinforce mechanical resistance to slip by means of projections. δ_f increases in proportion to pull-out load after relative slip is generated. Therefore, τ_b is more important factor rather than τ_{bmax} in pull-out test for lugged steel plate. It can be recognized from Fig.4 that τ_b is roughly in proportion to h and inverse proportion to d.

However, there are limiting factors in manufacturing of projection on flanges such as pressing capacity and temperature control during rolling process. On the basis of the test results and investigations, 3.5 mm and 19 mm have been adopted as lateral projection height and space on surface of deformed flange H-shapes, respectively.

Sign of specimen	Projection h (mm)	Projection d (mm)	Bond stress τ_b(MPa) δ_f=0.05 mm	Bond stress τ_b(MPa) δ_f=1.00 mm	Remark
A 0			2.2	2.4	Flat plate
A-1.5-a	1.5	7.5	10.1	14.5	Lateral lug
b	,,	15.0	8.6	15.5	,,
c	,,	22.5	6.0	13.8	,,
d	,,	30.0	5.0	10.9	,,
A-3.0-a	3.0	15.0	11.6	18.1	,,
b	,,	30.0	7.1	17.1	,,
c	,,	45.0	5.1	13.7	,,
d	,,	60.0	4.7	11.1	,,
A-4.5-a	4.5	22.5	10.3	18.2	,,
b	,,	45.0	7.5	16.3	,,
c	,,	67.5	7.2	16.2	,,
d	,,	90.0	6.8	13.4	,,
A-6.0-a	6.0	30.0	11.0	20.6	,,
b	,,	60.0	7.5	16.9	,,
c	,,	90.0	7.0	15.6	,,
DFH	3.5	20	11.5	20.5	Deformed flange
D51	3.5	15	8.4	15.5	Deformed bar

Table 1 Results on pull-out test

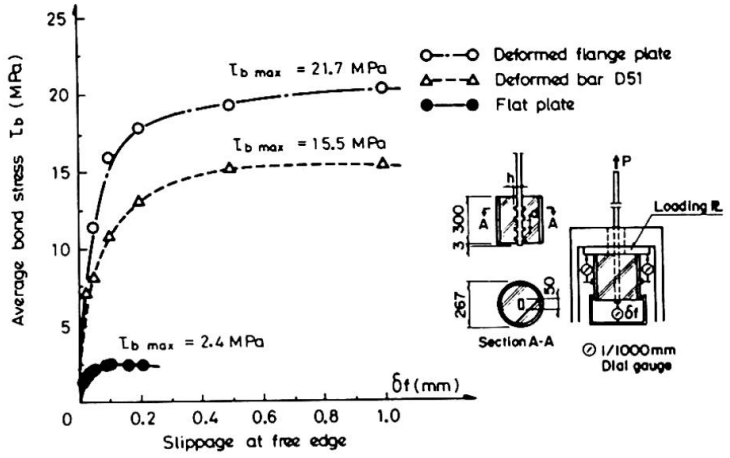

Fig. 3 Average bond stress and slip curves

3. CALCULATION OF WORKING STRESS AND ULTIMATE STRENGTH

3.1 Calculation of Neutral Axis and Shearing Stress

When concrete is sufficiently bonded to steel girder and they form the unit construction, it is an usual practice to neglect the tensile stress of concrete and obtain the stress of the composite materials on the basis of the converted sectional area method in which the compressive concrete is transposed to that of steel by using the elastic modulus ratio.

The distance X from the upper extreme edge of concrete to the

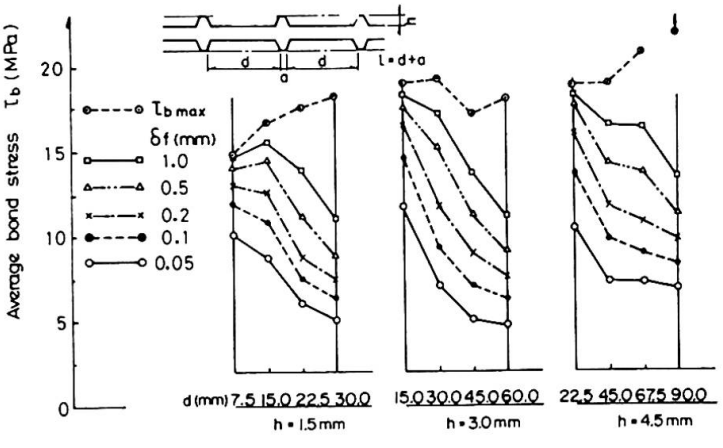

Fig. 4 Relation between average bond stress and projection height & space

neutral axis is obtained by

$$X = \frac{n \cdot A_s}{B}\left(-1+\sqrt{1+\frac{2 \cdot B \cdot g_s}{n \cdot A_s}}\right) \quad (1)$$

where B: Lateral distance between deformed flange T-shapes (cm)
A_s: Sectional area of steel girder (cm^2)
g_s: Distance from upper extreme edge of concrete to the center of gravity of steel grider (cm)
n: The elastic modulus ratio of steel to concrete

Next, the moment of inertia of the composite section I_v is obtained by

$$I_v = \frac{B \cdot X^2}{3n} + I_s + A_s(g_s - X)^2 \quad (2)$$

where I_s: The moment of inertia of steel girder (cm^4).

Assuming that horizontal shearing force is transmitted by projection on the upper flange, shearing stress τ_d is given by

$$\tau_d = \frac{Q_c \cdot S_d}{I_v \cdot b_f} \quad (3)$$

where Qc: Statical moment of area converted into steel on the compression side of concrete (cm^3)
b_f: Width of upper flange (cm)
S_d: Shearing force (N)

3.2 Calculation Formulas of Ultimate Strength

3.2.1 Assumptions

(1) Ultimate stress distribution of steel and concrete section is assumed to be rectangular shape.
(2) Tensile stress of concrete is neglected.
(3) The sectional area of steel is not subtracted from that of concrete.
(4) Ultimate strengths of concrete and steel are definited as 85% of design strength of concrete and nominal yield point of steel, respectively.

3.2.2 Calculation Formulas for X_p, M_u and τ_u

The distance X_p from the upper extreme edge of concrete to the neutral axis at the failure stage is obtained from the following equilibrium equation,

$$\Sigma A_i \cdot \sigma_i = 0 \quad (4)$$

The ultimate resisting moment M_u is calculated as follows,

$$M_u = \Sigma A_i \cdot \sigma_i \cdot X_i \quad (5)$$

where X_i: the distance from the neutral axis to the center of gravity of the divided sectional area A_i of steel girder, reinforcement and concrete.

The ultimate shearing stress τ_u on the upper flange projection is derived from the equilibrium equation at the failure stage and expressed as

$$\tau_u = \frac{0.85\sigma_{ck} \cdot B \cdot X_p \cdot S_u}{M_u \cdot b_f} \quad (6)$$

where S_u: The ultimate shearing force (N)
σ_{ck}: The design strength of concrete

4. EXPERIMENT OF COMPOSITE SLAB BRIDGE

4.1 The Purpose of Experiment

Static bending rupture test was conducted on the composite slab bridge with the aim of verifying the characteristics in the elastic range and the unification of the steel girder and slab concrete at the failure stage. High-cycle fatigue test was conducted on the other slab specimen with the aim of investigating the fatigue characteristics of composite slab under repeated loading.

4.2 The Dimensions of Specimen

The dimensions of composite slab specimen for static test are shown in Fig. 5. T-248 x 199 x 9 x 14 with projections were welded on the 12 mm thick bottom plate at a pitch of 40 cm in the longitudinal direction, D13 bars were arranged in the middle of the upper flange, and the slab depth was made 31 cm. In the specimen for fatigue test, the slab depth was made 21 cm and the bottom plate thickness was 8 mm, as shown in Fig. 6, in order to make the slab depth thinner than the lower limit of "Specification for Highway Bridges" in Japan and achieve economical cost performance. In both specimens, the maximum size of coarse aggregate was 25 mm, and the water cement ratio was 47%. Two kinds of ready mixed concrete having the design strength of 29.4 and 34.3 MPa were used for static and fatigue test specimen, respectively. An expansive admixture in a dose of 30 kg/m^3 was used to prevent cracking of concrete due to dry shrinkage.

4.3 Discussion

4.3.1 Static Bending Rupture Test

Fig. 7 shows the lateral distribution of bending stress at mid-span section when concentrated load 235 kN is applied to the center of the slab bridge. The experimental value is measured from the right-angle strain gauge, and the calculated value are obtained by the converted sectional area method in which the bending moment is obtained on the basis of the isotropical slab theory. The experimental value is nearly equal to the calculated value and rationally distributed over the entire width. Thus, the validity of the calculation method of working stress by using the isotropical slab theory and converted sectional area method has been verified.

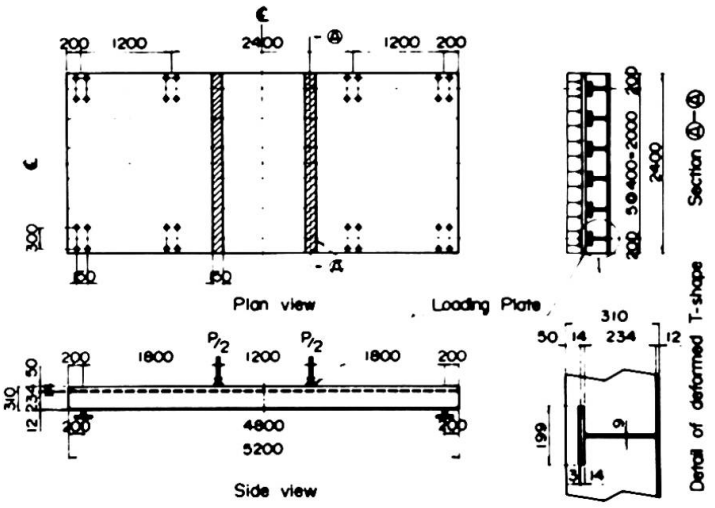

Fig. 5 Dimensions of specimen for static test

Fig. 8 shows the relation between bending moment and strain at the cross section of the mid-span when 2-point concentrated line loads are applied. This figure has verified that (i) the experimental values are approximately equal to the calculated ones up to the loading stage P_{ds} where the calculated stress of the bottom plate

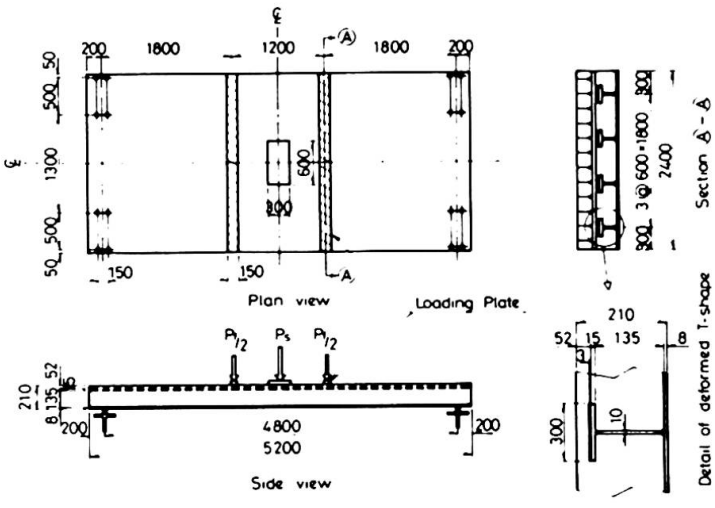

Fig.6 Dimensions of specimen for fatigue test

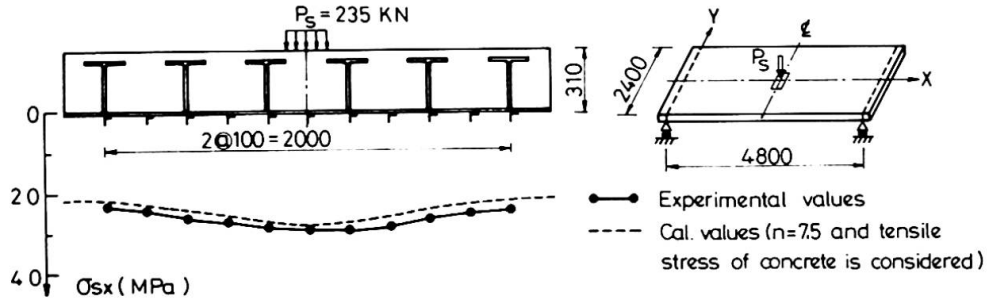

Fig. 7 Lateral distribution of tensile stress at mid-span section

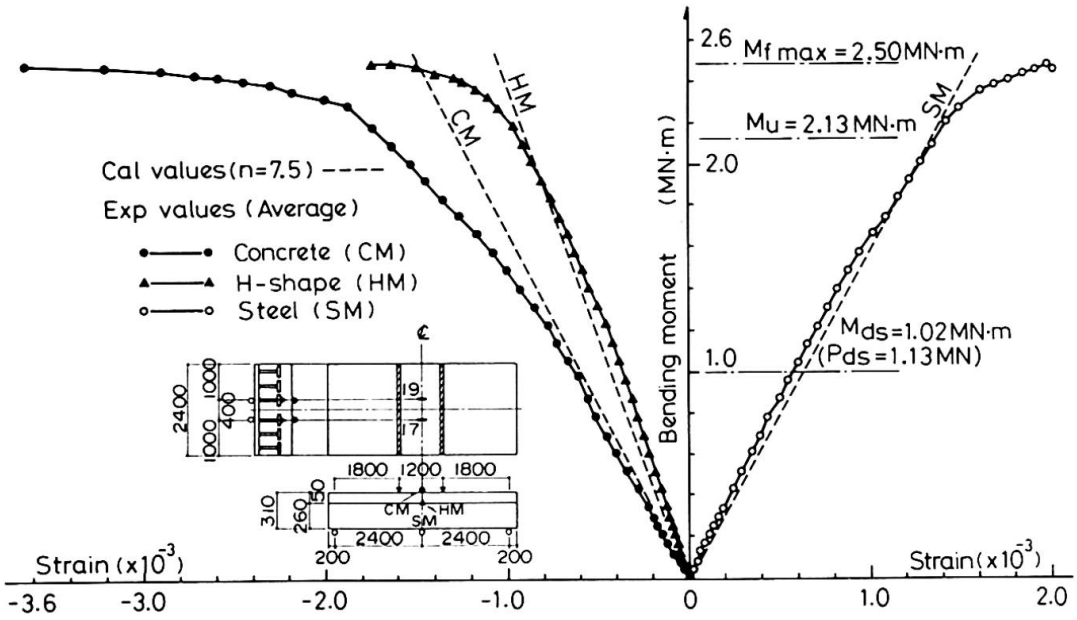

Fig. 8 Relation between bending moment and strain at mid-span section

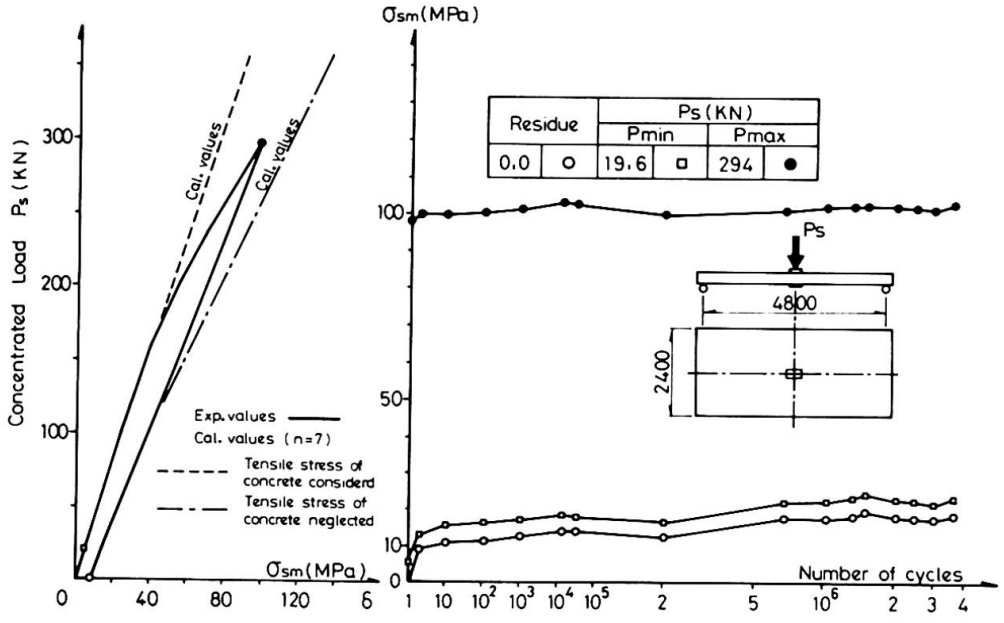

Fig. 9 Relation between number of cycles and tensile stress at mid-span section on fatigue test

corresponds to the allowable tensile stress, (ii) the ultimate bending compressive strain of concrete is 3.6×10^{-3} which is larger than that of conventional reinforced concrete, (iii) the ultimate bending moment is 2.50 MN·m which is about 1.2 tomes the calculated ultimate moment of 2.13 MN·m obtained from the Eq. (5) and (iv) the steel girder and slab concrete remain in the unit construction at the failure stage.

4.3.2 Fatigue Test

Fig. 9 shows the relation between the stress of the bottom plateand the number of cycles of repetition when a concentrated load is applied to the center of the slab bridge. Up to the load of 157 KN in the initial loading, the experimental value was nearly equal to the calculated one which has been obtained by considering the tensile stress of concrete, but thereafter, the experimental value became asymptotically to the calculated value in which the tensile stress of concrete was neglected. Under repeated load range from 19.6 to 294 KN, residual stress after the initial loading slightly increased, but no increase in the amplitude of stress range was observed, and the residual stress remained at a nearly constant level during 3.6 million cycles of repetition.

5. THE DESIGN

5.1 Design in General

Load: Calculation of sectional force by live load shall conform to "Specification for Highway Bridges" (called Spec.), III, 6.4. Namely, the design bending moment at the mid-span due to live load can be calculated by assuming that the total load (a uniform load of 3.43 KPa is applied to the whole width of the sidewalk and the principal L load is applied to the whole width of the roadway) will be uniformly borne by main girders.

Impact coefficient: The formulas applicable to reinforced concrete bridges given in Spec. Table 2.1.7 shall be applied.

Main materials: Atmospheric corrosion resisting steel (SMA 41W and SMA 50W) shall be used for the bottom plates, and SM50Y for the deformed flange T-shapes. For the slab concrete, the design strength shall be 26.5 MPa or above, and expansive concrete with the unit admixture quantity of 30 kg/m shall be used.

Determination of cross section: Sectional stress can be calculated according to Spec., II, Chapter 9 "Composite Girders". Namely. calculation shall be made on the assumption that the dead load of steel girder and slab concrete will be borne only by steel girder, and the dead load after placing concrete and the live load will be borne by the complete composite section. Stress variation due to creep and dry shrinkage of the slab concrete can be calculated by Spec., II, 9.2.6 and 9.2.8, respectively.

Shearing stress: Shearing stress at the projection on the upper flange can be calculated by Eq. (3). The allowable shearing stress shall be the same as that of deformed bar.

Limit of deflection: The maximum deflection due to live load shall be the value of 1/600 or below.

5.2 Standard Design

Road bridges having a span of 10 to 24 m were designed for three cases, the 2nd class bridge having the roadway width of 6 m, the 1st class bridge having the roadway width of 7 m and the 1st class bridge having the roadway width of 6.5 m and the sidewalk width of 2 m. The span/depth ratios of these standard design bridges are more than 33 as shown in Fig. 10.

6. CONCLUSION

As the result of experimental and analytical investigations on the composite slab bridge using deformed flange T-shapes, following concepts were obtained.

(1) Working stress can be obtain by the calculation method based on the isotropical slab theory and converted sectional area method.
(2) The steel girder and slab concrete retain a co-operative behavior even at the failure stage owing to the effect of projections on the upper flange.
(3) The composite slab can satisfactorily endure untill 3.6 million cycles of 294 KN repeated loading, which corresponds to three times as large as the design wheel load.
(4) The depth of the composite slab bridge can be greatly lower compared with the depth of steel plate girders and prestressed concrete bridges.

Since the commencement of sales for this slab bridge in the fall of 1982, more than fifty bridges have already been designed and five bridges have been completed, including four Bridges (see Figs.11 & 12) as a result of river improvement and another composite slab bridge used as the top slab of a tunnel (see Fig. 13).

In the future, the guide of the design and construction for curved bridges will be established and hollow type composite slab bridge will be developed for longer span.

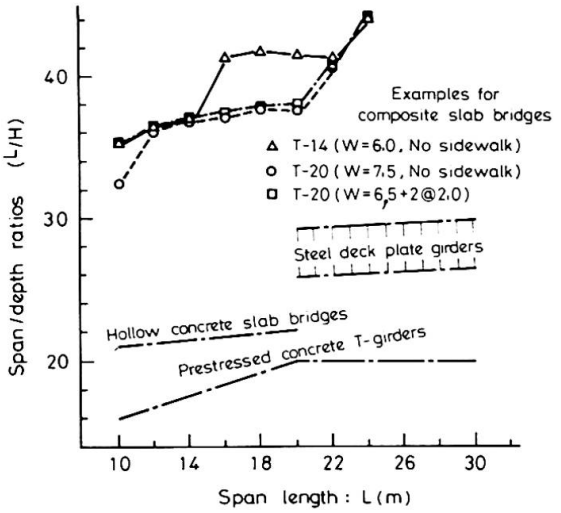

Fig. 10 The span/depth ratios for road bridges in Japan

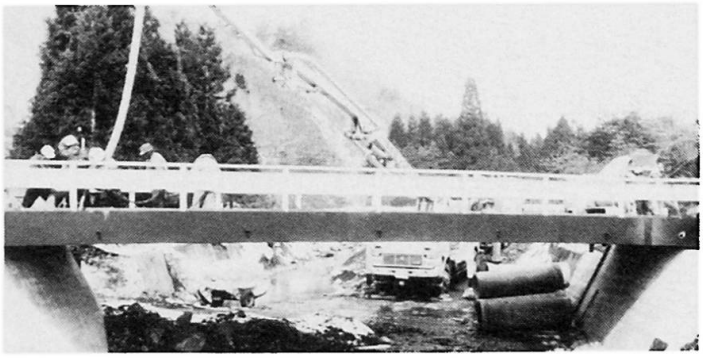

Fig. 11 Yachi-nakagawa bridge (L/H=42)

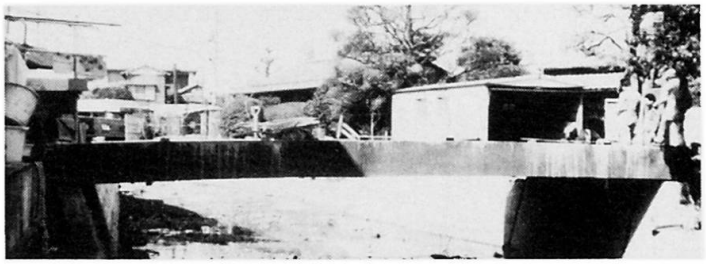

Fig. 12 Sengen-uemachi bridge (L/H=33)

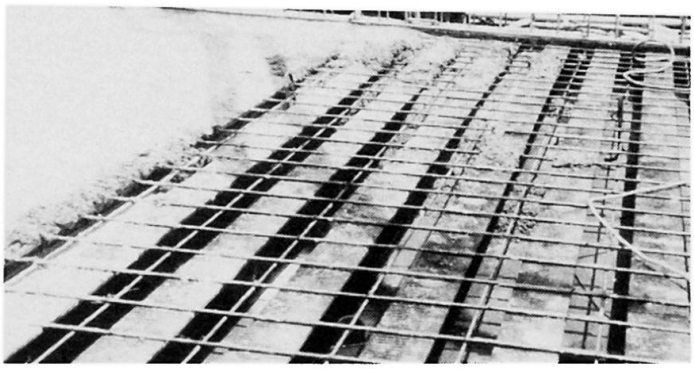

Fig. 13 The top slab of a tunnel (L/H=23)

REFERENCES

1. YAMASAKI T. et al., Studies on Fatigue Characteristics of Large Diameter Deformed Bar D51 in Axial Loads and Reinforced Concrete Beams. Trans. of JSCE, Vol. 10, pp.301 ∿ 302, 1978

2. SATO M. et al., Introducing Composite Structures using Newly Developed Checkered Steel Pipe and Deformed Flange H-shapes, KAWASAKI STEEL TECHNICAL REPORT No. 5, pp.94 ∿ 104, May 1982